

An Approach for Self-Powered Cardiovascular Monitoring Based on Electromagnetic Induction

G. Karageorgos, C. Manopoulos, A. Kiourti, A. Karagiannis, S. Tsangaris, and K. S. Nikita, *Senior Member, IEEE*

Abstract—Though medical implantable devices are highly suitable for continuous and real time patient monitoring, their battery replacement is a costly and complicated procedure. To extend the functional life of medical implants, energy harvesting methods have been investigated that convert the motions of the cardiovascular system to electrical energy. In this paper, we present the potential of such an energy harvester to operate as a sensor for cardiovascular parameters estimation, thus enabling the realization of a novel self-powered implantable cardiovascular monitor. This energy harvester is based on electromagnetic induction and exploits a conductive coil that moves along with an artery inside a magnetic field, applied by two permanent ring magnets. A similar device was fabricated and in order to test it, an experimental setup was developed that simulates arterial wall motion. Our in-vitro experiments demonstrated that the voltage induced in the coil is linearly related with arterial wall velocity and heart rate (coefficient of determination $R^2 > 0.99$). Moreover, the induced voltage was associated with blood pressure and the deforming artery's radius through a second order polynomial fit ($R^2 > 0.99$).

Index Terms—arterial wall motion, blood pressure sensor, cardiovascular monitoring, electromagnetic induction, energy harvesting, medical implantable devices, self-powered sensor.

I. INTRODUCTION

Hypertension (HTN), the abnormal elevation of blood pressure (BP), is a primary risk factor for cardiovascular disease. The latter is the leading cause of death worldwide accounting for at least 17.3 million deaths per year [1], [2]. Stroke, kidney failure and vision loss can also be some of its consequences when left untreated [3]. HTN is labeled as the “silent killer” as it usually has no symptoms, thus affecting a patient without even noticing [4]. Approximately one third of the U.S. residents have HTN, and 33% of them are not aware of their condition [1]. BP measurements are therefore necessary for the diagnosis and appropriate management of

HTN, as well as the prevention of its negative health effects. Heart rate is another physiological parameter that indicates the state of the cardiovascular system and can be used for HTN diagnosis [4].

Both invasive and non-invasive methods can be used to measure BP. Use of cuff-based oscillometric monitors is a common practice to measure BP [4]. However, these monitors do not provide continuous measurements and are not convenient for the patient given that regular cuff placement is required. The Photoplethysmography (PPT) and Pulse Transit Time (PPT) methods enable non-invasive, cuffless and continuous (BP) monitoring [4], [5]. However, non-invasive methods do not offer high accuracy and precision [6]. Intra-arterial catheters are a standard invasive technique that provides highly accurate pressure measurements, but they involve the risk of infection, distal vessel occlusion and hemorrhage [7].

Medical implants have proven to be highly suitable for patient monitoring applications. Advances in microelectronics and microsystems technology have enabled the development of low cost and small size implantable devices that integrate sensors with wireless telemetry capabilities, and provide accurate, long term, continuous and real time measurements of physiological signals, without requiring any action from the patient.

Though medical implantable devices exhibit several advantages, their power supply typically relies on batteries, which have limited lifetime and must be replaced through surgical procedure, exposing the patient to health risks. To this end, there has been an effort to minimize the energy requirements of such devices. Moreover, Energy harvesting has been investigated as an alternative to power implanted devices and extend their functional life. Energy sources such as the thermal energy inside the body, solar energy, kinetic energy of internal organs, chemical energy of glucose, RF radiation energy and ultrasound have demonstrated the feasibility to generate electrical power for implanted devices ([8] - [12]).

Among these energy sources, motions of the cardiovascular system are showing great promise for powering medical implants, since they are an inexhaustible source of mechanical energy which can be exploited to produce electrical power. For example, a device that uses thin PZT ribbons to convert the cardiac motion to electrical energy has been fabricated which generated power density per PZT area $1.2 \mu\text{W}/\text{cm}^2$ in vivo [13], while another energy harvester that generates electrical power from the beating heart through a mass imbalance oscillation generator has been developed, which

Paper submitted on 2 March 2017.

G. Karageorgos, A. Karagiannis and K.S. Nikita are with the School of Electrical and Computer Engineering, National Technical University of Athens, Zografos 15780, Greece (e-mail: gmkara@biosim.ntua.gr; akarag@mobile.ntua.gr; knikita@ece.ntua.gr).

C. Manopoulos and S. Tsangaris are with the School of Mechanical Engineering, National Technical University of Athens, Zografos 15780, Greece (e-mail: manopoul@central.ntua.gr; sgt@fluid.mech.ntua.gr).

A. Kiourti is with the Department of Electrical and Computer Engineering, Ohio State University, Columbus, OH, USA (e-mail: kiourti.1@osu.edu).

was able to produce 16.7 μW from the motion of a sheep's heart [14]. A mechanism to scavenge energy from arterial pulsation, based on electromagnetic induction that generated 42 nW in vitro has been proposed [15]. Furthermore, an energy harvesting device that employs a piezoelectric thinfilm to generate electrical energy from the motion of the aorta has been implemented, which extracted a maximum power of 40 nW in vivo and could also be used as an implantable sensor for BP monitoring [16]. For comparison, the power consumption of some typical medical implants with application to the cardiovascular system are provided in Table 1. The approach adopted in [16] can be quite beneficial to the functional life of a medical implant, given that its sensing system would not only provide pressure measurements, but it would also produce electrical energy for its power supply.

In this paper, we present the potential of the energy harvesting device proposed in [15] to operate as a sensor for cardiovascular system monitoring. This energy harvester uses a coil formed by conductive wire, which moves along with the artery inside the magnetic field applied by two permanent ring magnets, resulting in the induction of an alternating voltage. A similar device was fabricated and an experimental setup was developed that mimics arterial motion, by causing a periodic pressure excitation inside a silicon tube filled with water. The time waveforms of the output voltage of the electromagnetic transducer and the pressure inside the pulsating tube were obtained for different values of frequency and pressure amplitude, while the time waveforms of the deforming tube's radius and wall velocity were determined from the measured pressure via a mechanical analysis. In all cases, the output voltage had a periodic waveform of similar shape with the one of the tube's wall velocity, and a frequency equal to the applied pressure pulse, corresponding to the heart rate. An analysis of the measured data demonstrated that the voltage induced in the coil is linearly associated with the velocity of the arterial wall and the frequency of the pressure pulse. Moreover, the peak value of the induced voltage indicated a positive correlation with the corresponding pressure amplitude and the maximum deformation, which was modeled using a second order polynomial fit.

TABLE I
POWER CONSUMPTION OF MEDICAL IMPLANTS WITH APPLICATION TO THE
CARDIOVASCULAR SYSTEM [17]

Medical Implant	Power Consumption (μW)
Cardiac activity recorder	30-35
Current pacemaker	15-50
Leadless Pacemaker	1-10
Implantable cardioverter defibrillator	4-60
Blood pressure sensor	<10

II. SENSOR OVERVIEW & WORKING PRINCIPLE

The proposed sensor is based on an electromagnetic transduction mechanism, formerly developed for energy

harvesting from the motion of an artery. Its main components are two permanent ring magnets that are placed in parallel, and a coil that is positioned between them. The coil is formed with side loops, so that it can deform freely without limiting the artery's expansion. Fig. 1-(a) shows coil type 1, which is formed with three side loops and is the original coil used in [15], while Fig. 1-(b) illustrates coil type 2, which is an optimized design including one additional side loop. The main loop of the coil is aligned with the holes of magnets, and the device is placed around the artery as shown in Fig 1-(c).

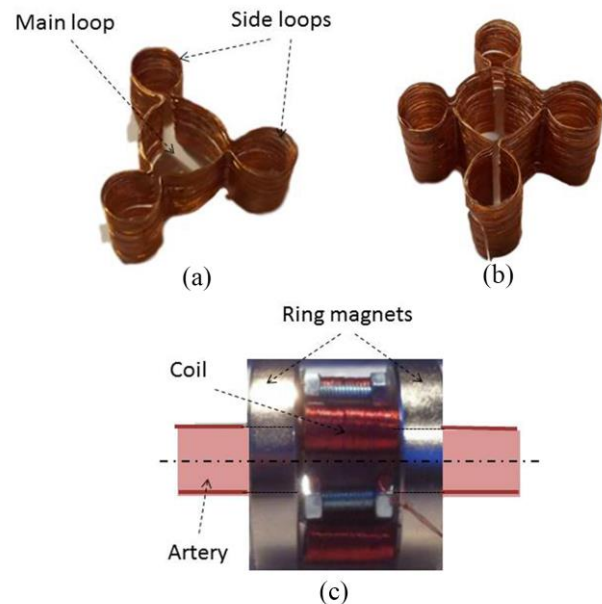


Fig. 1: (a) The flexible coil with three side loops that was used in a previous study (coil type 1). (b) Optimized flexible coil with four side loops (coil type 2). (c) The sensor under study.

The deformation of the artery causes the coil's main loop to move along with the arterial wall inside the magnetic field. As a result, an alternating voltage is induced across its terminals, which is proportional to the arterial wall's velocity. Fig. 2 depicts the motion of the coil during the artery's expansion, where the arrows denote the direction in which the coil deforms. Given that the side loops also move inside the magnetic field, they contribute to the voltage induction. Hence, coil type 2 is expected to produce higher voltage and power than coil type 1, due to its additional side loop.

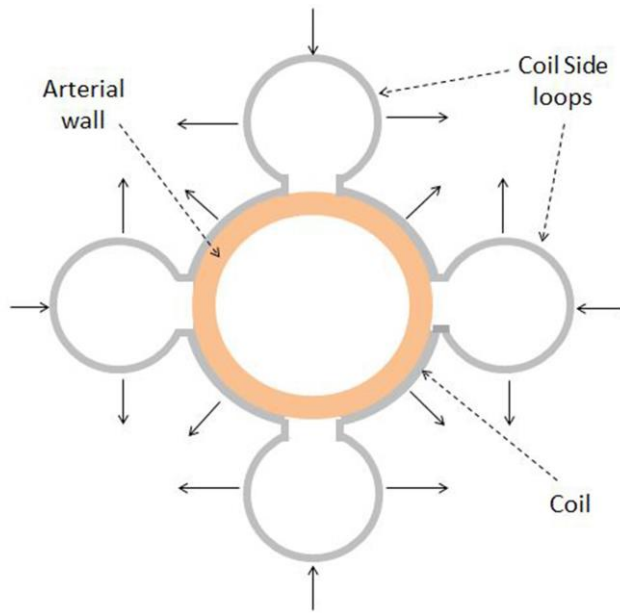


Fig. 2: Motion of the arterial wall and the coil during the artery's expansion.

III. THEORETICAL BACKGROUND

In order to demonstrate the potential of this particular energy harvesting device to operate as a sensor, a theoretical analysis was performed to associate its output voltage with the desired cardiovascular parameters. In this section, the expressions of the voltage induced in the coil and the generated power with respect to arterial wall velocity and displacement are presented, followed by a mechanical analysis that relates blood pressure with the pulsating artery's radius and velocity.

A. Output Voltage Estimation

Fig. 3 shows the proposed sensor along with the artery and the coordinate system employed in this study. The z -axis is parallel to the artery and the r -axis is along the radial direction, in which the arterial wall moves. The length of the magnets and the spacing between them are denoted by l and s , respectively. R_0 , d , R_{in} , R_{out} stand for the artery's undeformed inner radius, arterial wall's thickness, magnets' inner and outer radius, while $u_w(t)$ and $r(t)$ are the velocity and radial position of the arterial wall's outer layer as a function of time.

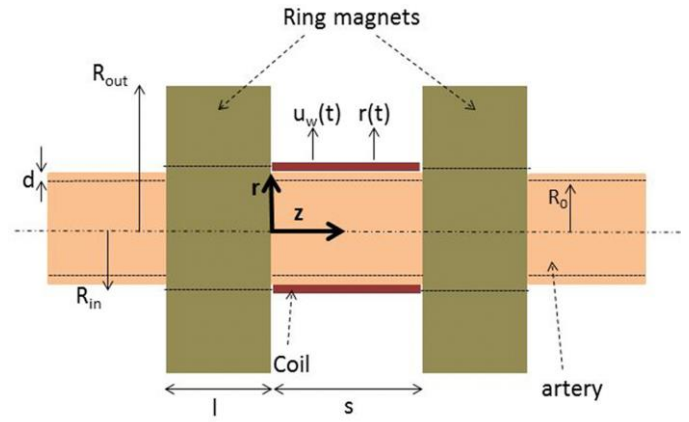


Fig. 3: Ring magnets, artery, coil and coordinates system.

In order to determine the output voltage of the sensor under study, the calculation of the magnetic field between the magnets is required. An axially magnetized ring magnet of differential length (dz) can be considered as the superposition of two infinitely thin solenoids, placed in parallel and circulated by opposite currents. The magnetic field of a ring magnet with length l can be estimated by integrating the magnetic field created by a similar magnet of differential length over l [15]. Fig. 4 depicts the direction of the magnetic field produced by a permanent ring magnet.

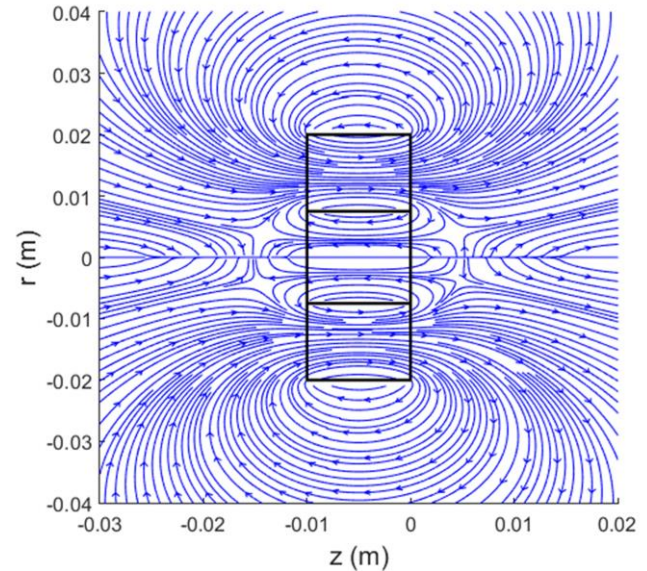


Fig. 4: Direction of the magnetic field produced by a permanent ring magnet.

Given that the artery deforms radially, only the z -component of the magnetic field $B_z(r,z)$ contributes to the voltage induction. In the case of two identical ring magnets placed in parallel at spacing s , the magnetic field at the space between them can be calculated at a given point (r,z) as the superposition of two permanent ring magnets as follows [15]:

$$B_z(r, z) = \int_z^{z+l} B_{dz}(r, z) dz + \int_{s-z}^{s-z+l} B_{dz}(r, z) dz \quad (1)$$

$B_{dz}(r,z)$ is the z-component of the magnetic field applied by an axially magnetized ring magnet with length, inner and outer radius dz , R_{in} and R_{out} , respectively and can be determined at a given point (r,z) by:

$$B_{dz}(r,z) = \frac{B_r}{2\pi} \frac{1}{\sqrt{(R_{out}+r)^2+z^2}} \left[E_{R=R_{out}} \frac{R_{out}^2-r^2-z^2}{(R_{out}-r)^2+z^2} + K_{R=R_{out}} \right] - \frac{B_r}{2\pi} \frac{1}{\sqrt{(R_{in}+r)^2+z^2}} \left[E_{R=R_{in}} \frac{R_{in}^2-r^2-z^2}{(R_{in}-r)^2+z^2} + K_{R=R_{in}} \right] \quad (2)$$

B_r is the magnets' remanence, while K and E are the complete elliptic integrals of the first and second kind, respectively. More extended analysis about the magnetic field calculation can be found in [15].

For the sake of simplicity, we assume a coil with cylindrical shape, without side loops, that is able to expand and contract radially along with the artery. Under this assumption, the coil and the outer layer of the arterial wall have the same radial position $r(t)$ and velocity $u_w(t)$, and the voltage induced in the coil is given by the following integral [15]:

$$V(t) = - \oint_c u_w(t) \times B_z(r(t),z) dl \quad (3)$$

where c is the curve defined by the coil. According to equation (3), the induced voltage depends on the radial velocity of each differential segment of the coil dl and the magnetic field at its given position $(r(t),z)$. The coil's maximum radial position corresponds to the maximum deformation of the arterial wall which is typically 10% of the artery's undeformed radius R_0 [15]. Considering that the magnetic field at a given axial position z does not vary significantly in the limited range of the radial position $r(t)$, the wall velocity is the dominant term in equation (3). Hence, a linear relationship is expected between the output voltage $V(t)$ and arterial wall velocity $u_w(t)$.

Based on equations (1)-(3), an analytical model was developed in Matlab R2015a to investigate the behavior of the device. The values that were assigned to the various parameters involving the properties and dimensions of the materials (magnets, wire, arterial wall) are the ones of the materials that we used for our prototype and our in vitro experiments and are specified in Table 2 of section IV. For our simulations, a sinusoidal outer arterial wall deformation [15] with a frequency of 1 Hz was considered,

$$r(t) = R_0 + d + \frac{R_{max}}{2} (1 - \cos(2\pi t)) \quad (4)$$

$$u_w(t) = \pi R_{max} \sin(2\pi t) \quad (5)$$

where the term (R_0+d) corresponds to the artery's undeformed outer radius and R_{max} is the maximum radial deformation of the artery.

Fig. 5 demonstrates the estimated peak voltage versus the peak arterial wall velocity for R_{max} ranging from 0.3 to 1.7 mm with a step of 0.1 mm. A linear relationship is observed according to our theoretical analysis, which we validate

through our in vitro experiments in the case of a coil with side loops in section V. The proportionality between the voltage and wall's velocity is a key relationship on which we based the scenario of the operation of this particular energy harvester as a sensor.

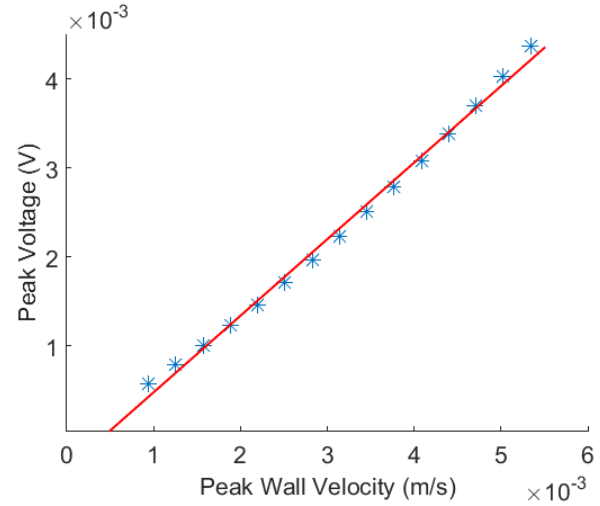


Fig. 5: The simulated diagram of the peak voltage versus peak wall velocity.

B. Power generation

The resistance of the coil (R_c) depends on the resistivity (ρ_w), length (L_w) and surface (A_w) of the wire and is given by:

$$R_c(t) = \rho_w \frac{L_w}{A_w} = \rho_w \frac{8Nr(t)}{d_w^2} \quad (6)$$

where N is the number of windings that form the coil and d_w is the diameter of the wire. The power transfer of the device is maximum when it functions with a load that matches the coil's resistance and is determined as follows [15]:

$$P_{max}(t) = \frac{\left(\frac{V(t)}{2}\right)^2}{R_c(t)} \quad (7)$$

To investigate the output power of the device with respect to the magnets' dimensions, a parametric study was performed based on equations (1)-(7), where R_{max} was set at a typical physiological value of 10%. Fig. 6-(a) presents the output power with respect to s for $l=10$ mm, $R_{in}=7.5$ mm, $R_{out}=20.5$ mm, while Fig. 6-(b) shows the output power as a function of R_{out} , l for $R_{in}=7.5$ mm and $s=20$ mm.

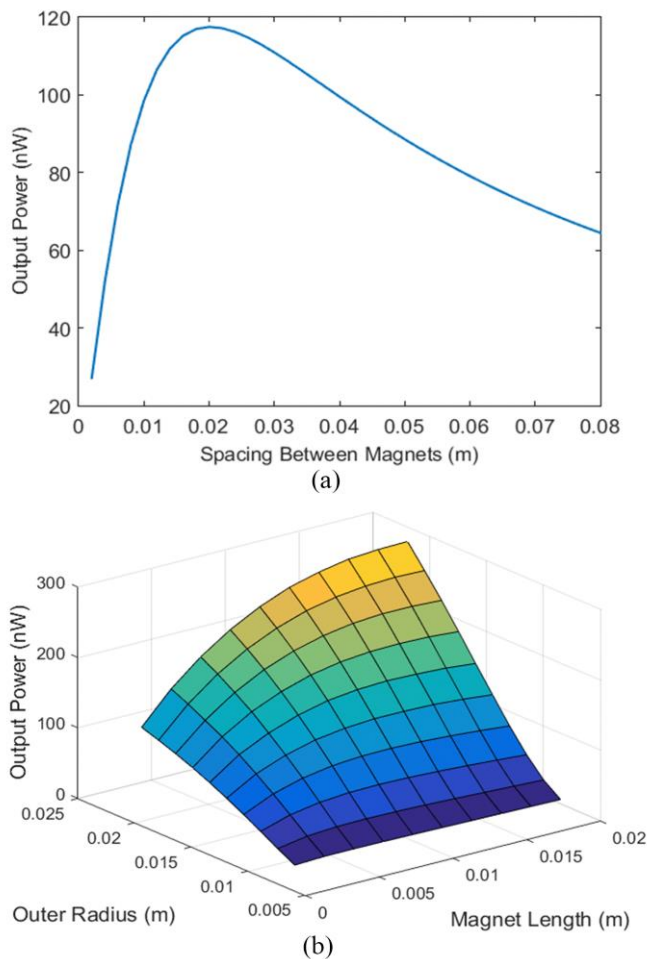


Fig. 6: Generated power with respect to (a) the spacing between the magnets (s) for $R_{out}=20.5$ mm, $R_{in}=7.5$ mm and $l=10$ mm and (b) the outer radius (R_{out}) and length (l) of the magnets for $s=20$ mm, $R_{in}=7.5$ mm.

C. Relationship between pressure and artery's motion

To show the potential use of this energy harvester as a blood pressure sensor, a relationship between its output voltage and blood pressure needs to be determined. The voltage induced in the coil is proportional the arterial wall velocity ($u_w(t)$). In the following, a mechanical analysis is presented to associate blood pressure with the artery's radius and wall velocity.

In our analysis, the artery is treated as an elastic, cylindrical tube, in which a periodic external pressure excitation is applied as illustrated in Fig. 7. We consider that far away from the excitation site, the tube deforms uniformly and its radius and internal pressure are invariable with respect to the axial position z.

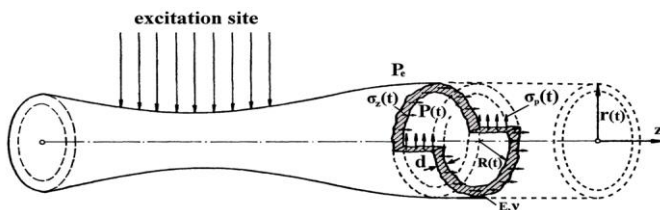


Fig. 7: Stress state of a cylindrical elastic tube's wall when transmural pressure is applied.

According to linear elasticity theory for thin elastic cylindrical tube walls, the peripheral and axial stresses σ_p and σ_z , respectively, are related to the peripheral and axial strains ε_p and ε_z by the following Hooke's law equations:

$$\varepsilon_p = \frac{\sigma_p}{E} - \frac{\nu\sigma_z}{E} \quad (8)$$

$$\varepsilon_z = \frac{\sigma_z}{E} - \frac{\nu\sigma_p}{E} \quad (9)$$

where E is the Young's modulus of the material that forms the wall and ν is Poisson's ratio. Assuming that the axial tube deformation is negligible, ε_z is zero and the following relationship is obtained for ε_p :

$$\varepsilon_p = \frac{(1 - \nu^2)\sigma_p}{E} \quad (10)$$

The peripheral wall stress is related with the pressure $P(t)$ inside the tube and the deforming tube's inner radius $R(t)$ through the Laplace law for cylindrical vessels as:

$$\sigma_p = \frac{(P(t) - P_e)R(t)}{d} \quad (11)$$

Where P_e is the environmental pressure and d is the thickness of the tube's wall. Moreover, by the definition of the peripheral strain we get:

$$\varepsilon_p = \frac{2\pi R(t) - 2\pi r R_0}{2\pi R_0} \quad (12)$$

where R_0 is the tube's undeformed inner radius. By combining equations (10), (11), (12) the following relationship between the pulsating tube's inner radius and its internal pressure is obtained:

$$R(t) = \frac{R_0}{1 - \frac{(P(t) - P_e)}{Ed} R_0 (1 - \nu^2)} \quad (13)$$

In the case of an artery, given that the velocity of the arterial wall is the first time derivative of the artery's radius ($u_w(t)=dr(t)/dt$), the output voltage of the proposed sensor is associated with blood pressure through the equations (3), (13). It is noted that the radial position of the coil's main loop $r(t)$ corresponds to the outer radius of the artery ($r(t)=R(t)+d$), where d is considered approximately constant during the artery's pulsation.

IV. FABRICATION

A. Sensor

The coils type 1 and type 2 illustrated in Fig. 1-(a), (b) were fabricated using enameled copper wire (resistivity $\rho=1.68 \cdot 10^{-8} \Omega \cdot m$) with a diameter (d_w) of 0.2 mm. We used Neodymium ring magnets, both axially magnetized, with remanence (B_r), length (l), inner (R_{in}) and outer (R_{out}) radius of 1.2 T, 10 mm, 7.5 mm and 20.5 mm, respectively. Non

magnetic screws made of stainless steel type 304 [18], were used as holders to place the magnets in parallel and at a spacing (s) of 20 mm. The spacing between the magnets was chosen to be 20 mm, because this value results in maximum power generation for the given magnets' dimensions, according to Fig. 6-(a). The total weight of the device was 188 g.

B. Experimental setup

To test the energy harvester and evaluate its performance as a sensor, the experimental setup shown in Fig. 8 was developed. The proposed setup simulates the arterial wall expansion and contraction. A cylindrical elastic tube made of platinum cured silicon with 6 mm undeformed inner radius (R_0), 1 mm wall thickness (d) and 1.97 MPa Young's modulus (E) was used as a mock artery. In order to perform pressure measurements, a tube system was formed by connecting the elastic tube with a rigid one made of plexiglas of the same radius. The one end of a catheter was then inserted to the rigid tube through a thin hole on its wall, while the other end was connected to an Edwards Truwave pressure disposable transducer integrated in a pressure monitoring kit [19]. The tube system was filled with water, and the ends of the tubes, the connection between the elastic and rigid tube, as well as the hole where the catheter was placed were air tightly sealed. All the air inside the tube system was removed through a valve connected to its one end and special care was taken so that there is no air or fluid leakage from inside the tube to the environment or vice versa.

Arterial wall pulsation was emulated by applying a periodic external pressure excitation to the flexible tube of the tube system through a motor-based compression device [20]. This device consists of a tube mounting groove in which a segment of the elastic tube is placed, and a 10 cm long oscillating reciprocating flat plate which periodically compresses and decompresses this segment. The oscillating flat plate is driven by a motor through a flywheel-rod system and the compression-decompression frequency can be adjusted through the motor's driver rotation speed. The device also includes a mechanism so that both the flexible tube mounting groove and the reciprocating flat plate can be moved in small steps up and down, adjusting the compression amplitude of the elastic tube. This way, the amplitude of the pressure pulse applied inside the tube system can be controlled. The tube's compression and decompression by the flat oscillating plate correspond to the cardiac systole and diastole, respectively.

The time waveforms of the pressure inside the tube system and the output voltage of the proposed sensor were synchronously sampled by using HBM Quantum^X MX440A Analog to Digital Converter (ADC) [21]. The output power was measured by connecting a load matching the resistance of each coil where the power transfer maximizes. The resistance of coil type 1 (R_{c1}) and type 2 (R_{c2}) was 8.2 and 10.3, respectively. Table 2 summarizes the parameters and dimensions of the materials that we used to fabricate the sensor and the experimental setup.

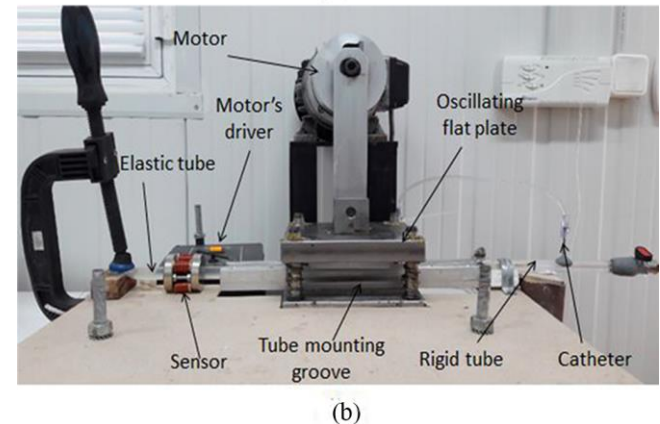
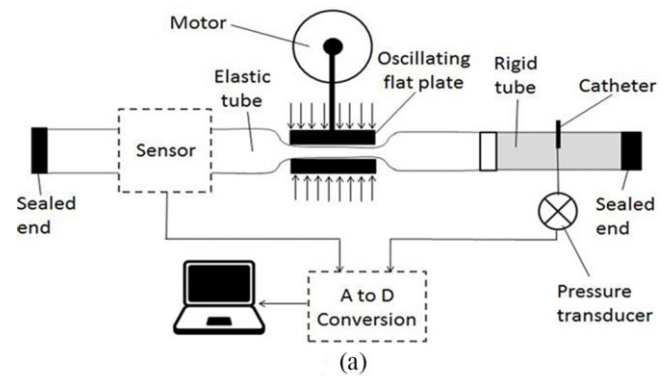


Fig. 8: (a) Diagram and (b) picture of the experimental setup for in-vitro testing. The elastic tube comes through the proposed sensor and is connected to a rigid tube. A catheter is inserted to the rigid tube which is connected to the pressure transducer. A pressure pulse is applied through partial compression and decompression of an elastic tube's segment. The time waveforms of the sensor's output voltage and the pressure inside the tube are synchronously obtained through analog to digital conversion.

TABLE II
PARAMETER VALUES FOR THE FABRICATED SENSOR AND EXPERIMENTAL SETUP

Parameter	Symbol	Values
Magnets's outer radius	R_{out}	20.5 mm
Magnets's inner radius	R_{in}	7.5 mm
Magnets' length	l	10 mm
Magnets' remanence	B_r	1.2 T
Spacing between magnets	s	20 mm
Copper wire diameter	d_w	0.2 mm
Copper wire resistivity	ρ	$1.68 \cdot 10^{-8} \Omega \cdot m$
Coil type 1 resistance	R_{c1}	8.2 Ω
Coil type 2 resistance	R_{c2}	10.3 Ω
Elastic Tube's undeformed inner radius	R_0	6 mm
Elastic tube's wall thickness	d	1 mm
Elastic tube's Young's modulus	E	1.97 MPa
Poisson's ratio	ν	0.49

V. RESULTS

A. Optimization

Firstly, coil type 1 and coil type 2 (Fig. 1-(a), (b), respectively) were tested in order to determine whether the additional side loop results in higher voltage and power generation. The amplitude of the pressure pulse was set so that a typical physiological arterial wall deformation could be reproduced, which is approximately 10% of the artery's undeformed radius. A 10% deformation of the tube was noticed at a systolic and diastolic pressure of 366.6 and 80.8 mmHg, respectively. It is noted that because the silicon tube used for our experiments is stiffer than a normal artery, the diastolic pressure was set on a higher than the physiological level, to cause sufficient deformation. At this pressure amplitude and for a frequency of 1.17 Hz, we measured the output voltage of each coil. The peak voltage of coils type 1 and type 2 was 1.5 and 1.8 mV, while their mean generated power was 8.4 and 10.9 nW, respectively. Due to its improved performance, coil type 2 was used for the following measurements.

B. Pressure response

In order to study the response of the proposed sensor with respect to the pressure and the tube's wall motion, the compression amplitude of the elastic tube was set at 15 different levels, each one resulting in a pressure pulse with different amplitude. For each of these compression amplitudes, the pressure inside the tube system and the voltage induced in the coil were measured. Equation (13) was used to calculate the inner radius of the deforming elastic tube from the pressure measurements. By differentiating the radius, the velocity of its wall was obtained. Fig. 9 shows the time waveforms of the pressure (Fig 9-(a)), the elastic tube's radius (Fig 9-(b)) and wall velocity (Fig 9-(c)) and the sensor's output voltage (Fig 9-(d)) for seven distinct compression amplitudes, at a frequency of 1.17 ± 0.03 Hz. The time waveform of the velocity is illustrated with opposite sign to demonstrate its proportionality with the voltage. It is noted that the distortion before the elevation of the wall velocity and output voltage in Fig. 9-(c), (d) is due to small vibrations caused by instabilities of the motor.

Fig. 10-(a) shows the peak open circuit voltage versus the peak velocity of the tube's wall, corresponding to 15 different values of pressure amplitude, along with a least squares linear fit. An excellent linearity is observed between these two quantities (coefficient of determination $R^2 = 0.997$), validating the theory, according to which the induced voltage is proportional to the velocity. The sensitivity can be defined as the slope of the applied linear fit, which is 288 mV/(m/s). Fig. 10-(b), (c) and (d) illustrate the diagrams of peak voltage against peak radius, peak wall velocity against pressure amplitude and peak voltage against pressure amplitude, along with their second-order polynomial fit with an R^2 of 0.996, 0.997 and 0.996, respectively.

We can observe that blood pressure, artery's deformation and arterial wall velocity can be determined through the output voltage of this particular energy harvesting device. The wall velocity is the easiest cardiovascular parameter to determine because of the presented linearity. Blood pressure and artery's radius can be calculated directly through the voltage by using

the second order polynomial approximations, or through the velocity by equations (3) and (13). Moreover, heart rate can be estimated from the frequency of the alternating voltage.

C. Frequency response

To investigate the frequency response of the proposed sensor, we fixed the elastic tube's compression amplitude to reproduce a typical arterial deformation of 10%, and measured the output voltage and power at different frequencies by adjusting the motor's rotation speed. Fig. 11 shows the output voltage and generated power against frequency.

The voltage and power increase as the frequency increases. This can be explained given that the voltage is proportional to the velocity of the tube's wall, which moves faster at higher frequencies. The linear fitting to the data illustrated in Fig. 11-(a) ($R^2 = 0.994$) suggests that the output voltage of the proposed sensor is linearly related with frequency, and thus, the heart rate.

D. Surrounding tissue emulation

Given that the aim of this sensing method is to form a medical implant, an experiment was run to test whether the surrounding tissue affects the voltage induction. The sensor under study was completely covered by minced meat, and a pressure excitation with frequency, diastolic and systolic pressure 1.28 Hz, 86.8 mm Hg and 364.9 mm Hg, respectively was applied inside the elastic tube. Afterwards, the minced meat was removed and the exact same pressure excitation was applied. No change of the proposed sensor's output voltage was observed. This can be explained because the only way for the tissue around the device to influence the induction is to change the static magnetic field at the space between the magnets where the coil deforms, and no significant changes are expected given the tissue's magnetic permeability is comparable to that of the air.

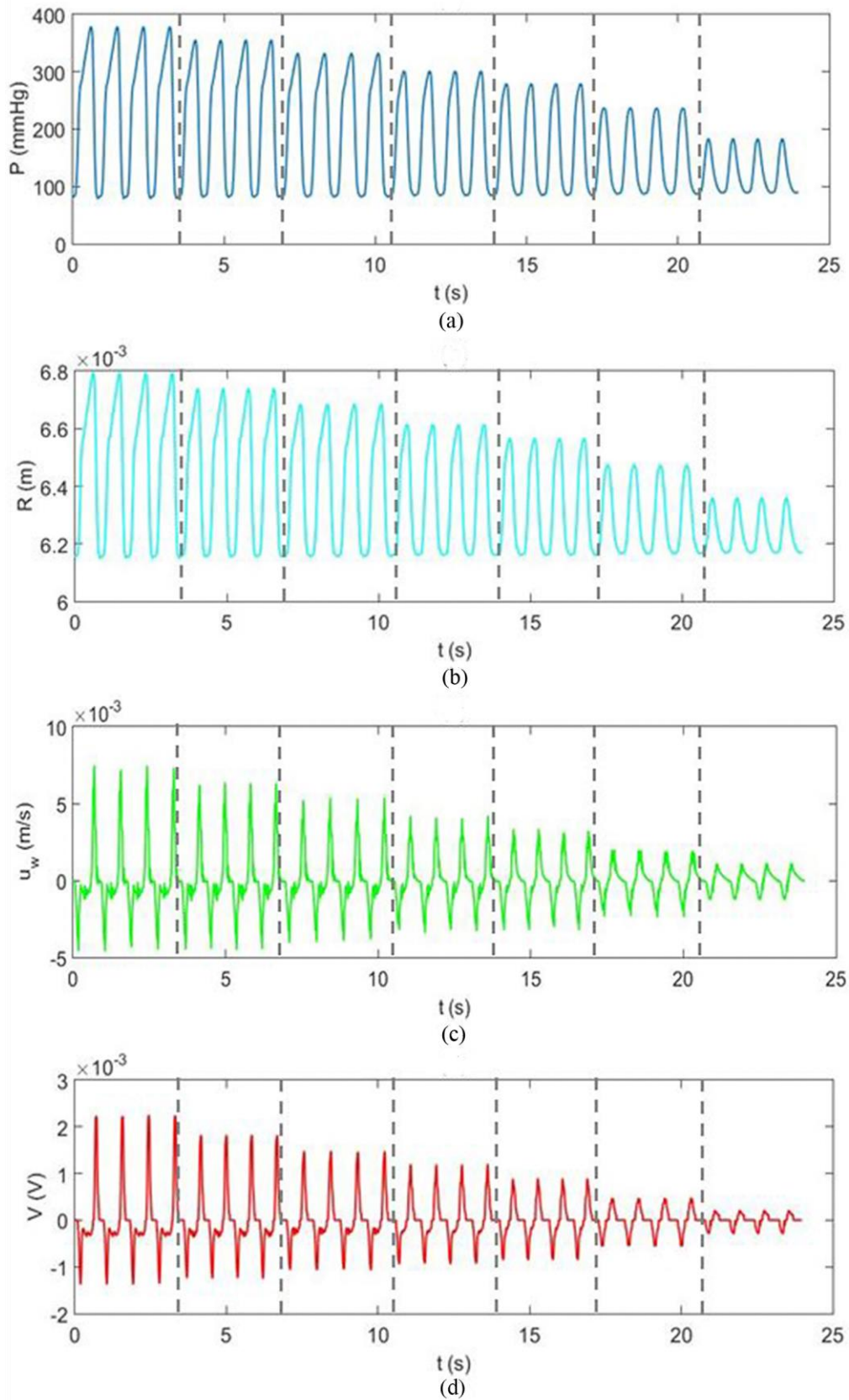


Fig. 9: Time waveforms of (a) measured pressure inside the tube, (b) elastic tube's radius, (c) elastic tube's wall velocity, (d) measured voltage of the proposed sensor.

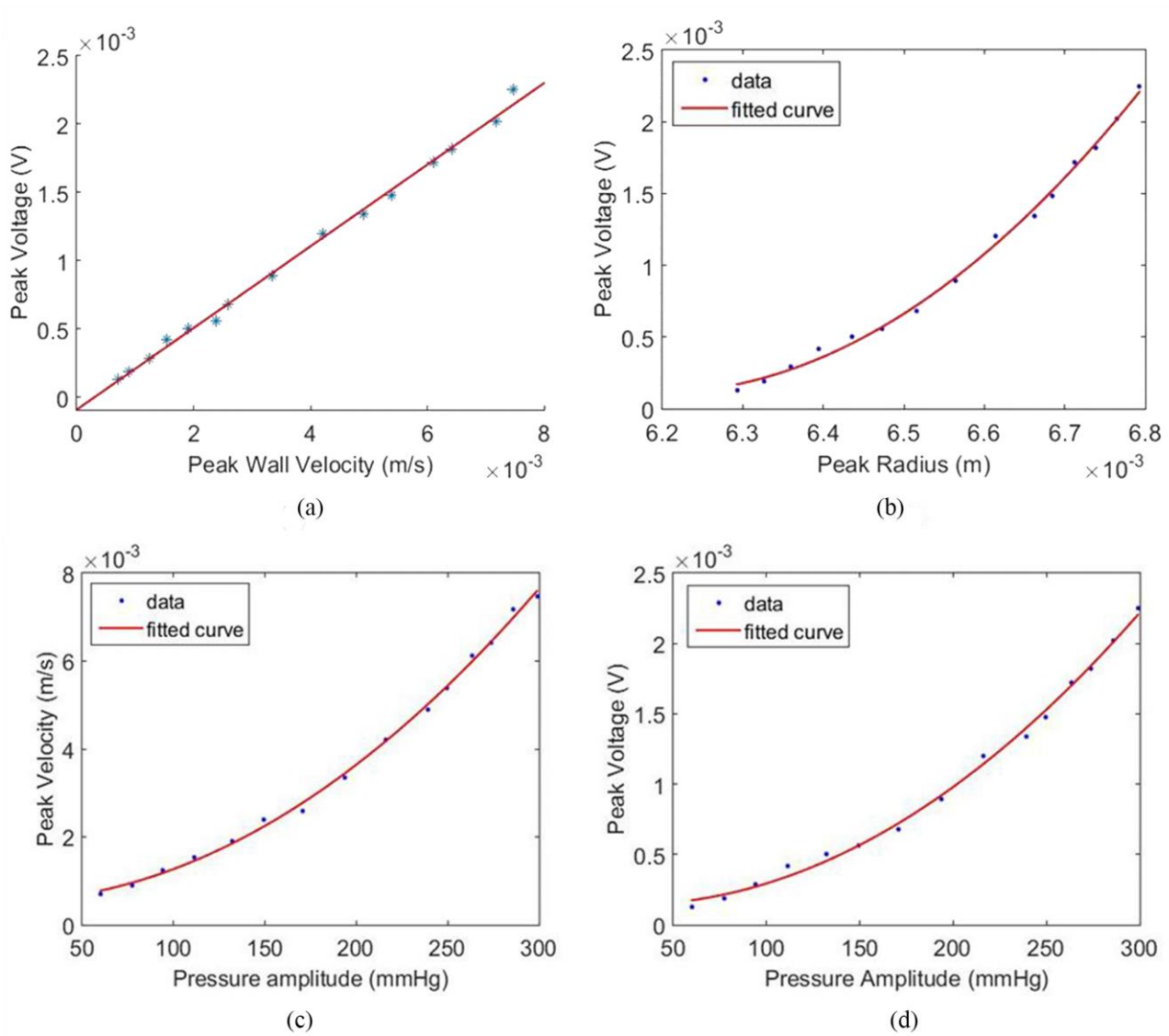


Fig. 10: (a) Peak voltage against the peak velocity of the tube's wall, (b) peak voltage against peak radius, (c) peak wall velocity against pressure amplitude and (d) peak voltage against pressure amplitude for a frequency of 1.17 ± 0.03 Hz

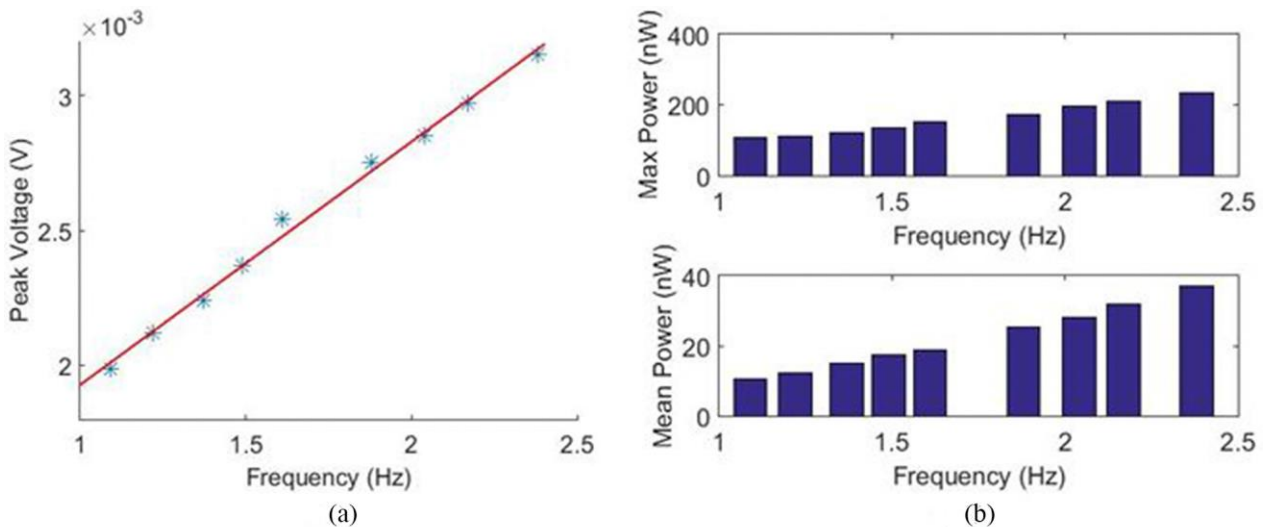


Fig. 11: (a) Voltage against frequency, (b) maximum and mean instantaneous power at a systolic and diastolic pressure of 366.6 and 80.8 mmHg respectively

VI. DISCUSSION

Our results indicate that the output voltage of this energy harvesting device can provide information on heart rate, blood pressure, arterial wall deformation and velocity, thus, if implanted, it can act as a sensor to provide continuous monitoring of the cardiovascular system.

The prototype fabricated in this study is intended to provide a proof-of-concept and is not destined for in vivo experimentation where smaller dimensions would eventually be required, so we did not determine target arteries for applying this device. In [15] though, the iliac artery with a diameter of 10mm was chosen as a possible implantation site.

An issue that might arise from a miniaturized version of this sensing device could be a reduction in the produced voltage and power. However, the prototype fabricated in [15] had smaller dimensions ($R_{out}=14$ mm, $R_{in}=5$ mm and $l=12$ mm), and was able to generate 42 nW mean power in vitro for a normal heart rate, which was higher than the corresponding power in our case. Even so, the output power of 42 nW is low compared to other energy harvesting methods and the power needs of medical implants. According to this study, the advantage of this mechanism is not due to its power generation, but because it can form a novel sensor, so emphasis was given on its relationship with cardiovascular parameters.

Two key factors affecting the device's output voltage and power are the volume of the wire moving inside the magnetic field, as well as the coil's flexibility given that the voltage is proportional to the arterial wall velocity, and a stiff coil would limit the artery's motion. In this study we presented that a coil geometry with an additional side loop resulted in higher voltage and power generation, and attributed this to the fact that more wire volume was included. Implementing a prototype with multiple coil layers would be an effective solution to the low energy generation. However, multiple coil layers would place additional mechanical constraint on the artery and limit its motion, reducing the sensor's sensitivity and generated power. Enhancing the coil's flexibility by experimenting with more flexible wire or alternative coil shapes in order to enable the construction of a multi-layered coil that will be able to move freely along with the artery, would be a possible future step of this work.

Unless an optimized design producing higher voltage is implemented, then for the use of this device as a sensor in its current state, given that the output voltage is in the range of a few mV, an amplification stage would probably be required for the post-processing and transmission of the measured signals.

In our in vitro experiments, the single-layer coils did not restrain significantly the motion of the elastic tube's wall. However the tube is stiffer than a normal artery and the applied pressure amplitude was set at a higher than the physiological level. In vivo testing would be required to determine the mechanical interaction of this device with the cardiovascular system. An analysis about the coil's stiffness, the scenario of multiple coil layers and the mechanical constraints on the artery can be found in [15].

The biocompatibility of the proposed sensor is a matter that needs to be investigated. It is possible that its implantation

would cause foreign body reactions to the surrounding tissue, as well as modify the mechanical properties of the artery (e.g. arterial stiffening caused by small inflammatory reactions), a fact that would affect the relationship between the voltage and the cardiovascular parameters. To address such issues, its design as an interponate has been proposed [15], where the sensor is placed around an artificial elastic graft instead of an artery, and the system is implanted through anastomosis. According to this idea, the device would consist of an outer biocompatible case like the ones commonly used for pacemakers and other medical implants (e.g titanium alloy housing), which would contain the magnets and the coil, and an elastic graft that would be placed inside the outer housing through the holes and the coil's main loop. Some examples of materials that would be appropriate for the fabrication of the graft in order to interact well with the blood are presented in [22-23].

If a design of this device proves feasible to be operated in vivo, then it could be implanted at the same time as surgical operations requiring anastomosis or other arterial interventions (e.g bypass) are performed. In case that its implantation is not possible, then it is a novel sensing method that could be used for applications other than biomedical, where fluid pressure inside elastic tubes, elastic tubes' wall velocity or displacement measurements are required.

Finally, another issue that might arise from the implantation of this device is the possible electromagnetic interference with other medical implants, or external sources. To counter such issues, the development of an appropriate biocompatible packaging for electromagnetic shielding would be necessary.

VII. CONCLUSION

In conclusion, we presented a novel sensing technique for cardiovascular monitoring. We demonstrated the feasibility of an energy harvester based on electromagnetic induction to provide information on heart rate, blood pressure, arterial wall deformation and velocity, which could potentially enable the development of a self-powered medical implant. The future steps of this research would involve the development of an optimized design of this device increasing the produced voltage and power, a study for its in vivo operation and its integration with the circuitry required for the processing and transmission of the measured signals.

REFERENCES

- [1] Merai, Rikita. "CDC Grand Rounds: A Public Health Approach to Detect and Control Hypertension." *MMWR. Morbidity and Mortality Weekly Report* 65 (2016).
- [2] American Heart Association. Available: http://www.heart.org/idc/groups/ahamah-public/@wcm/@sop/@smd/documents/downloadable/ucm_480086.pdf
- [3] Mayo Clinic. Available: <http://www.mayoclinic.org/diseases-conditions/high-blood-pressure/in-depth/high-blood-pressure/art-20045868>
- [4] Taha, Zahari, Lum Shirley, and Mohd Azraai Mohd Razman. "A review on non-invasive hypertension monitoring system by using photoplethysmography method." *Movement, Health & Exercise* 6.1 (2017).

- [5] Nikita, Konstantina S., ed. Handbook of biomedical telemetry. John Wiley & Sons, Chapter 4, 2014.
- [6] Yu, Lawrence, Brian J. Kim, and Ellis Meng. "Chronically implanted pressure sensors: challenges and state of the field." *Sensors* 14.11 (2014): 20620-20644.
- [7] Theodor, Michael, et al. "Subcutaneous blood pressure monitoring with an implantable optical sensor." *Biomedical microdevices* 15.5 (2013): 811-820.
- [8] Pfenniger, Alois, et al. "Energy harvesting from the cardiovascular system, or how to get a little help from yourself." *Annals of biomedical engineering* 41.11 (2013): 2248-2263.
- [9] Hannan, Mahammad A., et al. "Energy harvesting for the implantable biomedical devices: issues and challenges." *Biomedical engineering online* 13.1 (2014): 79.
- [10] Stetten, F. V., et al. "A one-compartment, direct glucose fuel cell for powering long-term medical implants." *Micro Electro Mechanical Systems, 2006. MEMS 2006 Istanbul. 19th IEEE International Conference on. IEEE, 2006.*
- [11] Haeberlin, Andreas, et al. "The first batteryless, solar-powered cardiac pacemaker." *Heart rhythm* 12.6 (2015): 1317-1323.
- [12] Song, S. H., A. Kim, and B. Ziaie. "Omnidirectional ultrasonic powering for millimeter-scale implantable devices." *IEEE Transactions on Biomedical Engineering* 62.11 (2015): 2717-2723.
- [13] Dagdeviren, Canan, et al. "Conformal piezoelectric energy harvesting and storage from motions of the heart, lung, and diaphragm." *Proceedings of the National Academy of Sciences* 111.5 (2014): 1927-1932.
- [14] Zurbuchen, Adrian, et al. "Energy harvesting from the beating heart by a mass imbalance oscillation generator." *Annals of biomedical engineering* 41.1 (2013): 131-141.
- [15] Pfenniger, Alois, et al. "Design and realization of an energy harvester using pulsating arterial pressure." *Medical engineering & physics* 35.9 (2013): 1256-1265.
- [16] Cheng, Xiaoliang, et al. "Implantable and self-powered blood pressure monitoring based on a piezoelectric thinfilm: Simulated, in vitro and in vivo studies." *Nano Energy* 22 (2016): 453-460.
- [17] Deterre, Martin. *Toward an energy harvester for leadless pacemakers.* Diss. Paris 11, 2013.
- [18] AK Steel Corporation, www.aksteel.com. Available: http://www.aksteel.com/pdf/markets_products/stainless/austenitic/304_304l_data_bulletin.pdf
- [19] Edwards Lifesciences. Available: http://www.dcdproducts.com.ar/documentos/50/80_TrWave%20Sensor%20Brochure.pdf.
- [20] C. Manopoulos, "A study of pumping phenomena for biomedical applications by means of fluid flow interaction with a moving body", Ph.D. Thesis (in Greek), pp. 392, National Technical University of Athens, 2009.
- [21] HBM (Hottinger Baldwin Messtechnik GmbH). Available: <https://www.hbm.com.pl/pdf/b2925.pdf>.
- [22] Huber, Birgit, et al. "Blood-Vessel Mimicking Structures by Stereolithographic Fabrication of Small Porous Tubes Using Cytocompatible Polyacrylate Elastomers, Biofunctionalization and Endothelialization." *Journal of functional biomaterials* 7.2 (2016): 11.
- [23] Ravi, Swathi, and Elliot L. Chaikof. "Biomaterials for vascular tissue engineering." *Regenerative medicine* 5.1 (2010): 107-120.



Grigorios Marios Karageorgos received his Diploma from the School of Electrical & Computer Engineering, National Technical University of Athens (NTUA), Greece, in 2016 and majored in electronic engineering. His undergraduate thesis focused on energy harvesting from the cardiovascular system with application to medical implants.

He is currently a member of the BIOmedical Simulations and IMaging laboratory (BIOSIM) of NTUA and working on a novel method for cardiovascular monitoring. His research

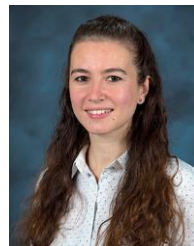
interests include energy harvesting and sensing systems for biomedical applications.



Christos Manopoulos received the Diploma degree in Mechanical Engineering from the School of Engineering at the University of Patras, Greece, in 1995, the M.Sc. and the Ph.D. degrees in Biomedical Engineering in 1999 and 2009, respectively, through a European Postgraduate Programme from the University of Patras, (School of Health Sciences, Faculty of Medicine) and the National Technical University of Athens, (School of Mechanical Engineering, School of Electrical & Computer Engineering), Greece.

He is currently a Senior Researcher and Laboratory Teaching Staff of biofluid mechanics in Fluids Section in School of Mechanical Engineering at the National Technical University of Athens, Greece. He has authored or coauthored more than 50 journal and conference papers. His research interests include theoretical, computational and experimental methods on biofluid mechanics, unsteady oscillating flows, fluid analysis, investigation and design of biomedical systems, devices and equipment related to biofluid mechanics technology, development of biofluid mechanics models in technology and living organisms (normal and pathological conditions), valveless pumping, peristaltic pumps, simulation and prototyping of medical devices and machines.

Dr. Manopoulos is a reviewer in several scientific journals. He has participated in scientific committees and has completed several projects in his research area. He has received a scholarship by the State Scholarships Foundation of Greece for his PhD, a Doctoral Research award in 2009 and several awards for some of his research publications.



Asimina Kiourti (S'10–M'14) received the Diploma degree in electrical and computer engineering from the University of Patras, Greece, in 2008, the M.Sc. degree in technologies for broadband communications from University College London, U.K., in 2009, and the Ph.D. degree in electrical and computer engineering from the National Technical University of Athens, Greece, in 2013.

She is currently an Assistant Professor of Electrical and Computer Engineering at The Ohio State University, Columbus, OH, USA. She has authored or coauthored more than 100 journal and conference papers and seven book chapters. Her research interests include medical sensing, antennas for body area applications, RF circuits, bioelectromagnetics, and flexible textile-based electronics.

Dr. Kiourti is Associate Editor for the IEEE Transactions on Antennas and Propagation. She has received several awards and scholarships, including the IEEE Engineering in Medicine and Biology Society (EMB-S) Young Investigator Award for 2014, the IEEE Microwave Theory and Techniques Society (MTT-S) Graduate Fellowship for Medical Applications for

2012, and the IEEE Antennas and Propagation Society (AP-S) Doctoral Research Award for 2011.



Dr. Alexandros Karagiannis received his Diploma from the Department of Electrical and Computer Engineering, National Technical University of Athens. He completed his diploma thesis on "Methods for Coronary Stenosis Detection". In February 2011 he completed his studies (M.Sc.) in the European Postgraduate Programme on

Biomedical Engineering. In 2012 he defended his PhD thesis on "Methods and Techniques for Energy Consumption Monitoring and Algorithm Modeling for Biomedical Signal Processing on Wireless Sensor Networks".

His main research interest is focused on body sensor networks, biomedical signal processing, and energy consumption optimization techniques and energy harvesting in wireless sensor networks. He has developed innovative solutions on water consumption monitoring based on energy harvesting from water flow and cardiovascular stenosis detection solution both awarded in national and international innovation competitions.



Sokrates Tsangaris (Dr techn. Professor emer.) received the Diploma degree in Mechanical and Electrical Engineering from the National Technical University of Athens (N.T.U.A.), Greece, in 1972, the Ph.D. (Dr techn.) in Aerodynamics from the Mechanical Engineering Faculty of the Technical University of Vienna, Austria, in 1976,

in the area of Transonic Aerodynamics.

For four years he joined the Biofluid Section of the Technical University of Vienna in 1975, where he worked as Research Assistant and Research Associate in the field of modeling blood flows in arteries and physiological measurements. In the period 1981-1997 he has been a Postdoctoral fellow, Lecturer, Assistant Professor and Associate Professor in the Mechanical Engineering Department of the N.T.U.A.

He was for two months (1985) a visiting scientist in "Fachhochschule Muenchen" Germany and for three months (1987) a visiting Professor in the Technical University of Vienna Austria. During the period 1997-2016 he has been Professor in the Mechanical Engineering Department of the N.T.U.A and Director of the Lab of Biofluid Mechanics and Biomedical Engineering. Since September 2016 he is nominated Professor Emeritus of N.T.U.A.

Professor Tsangaris research and working areas include fluid mechanics in general, biofluid-mechanics, biomedical engineering and theoretical aerodynamics, while his teaching experience is on fluid mechanics, biofluid-mechanics, aerodynamics, and biomedical engineering. He has been the supervisor of twenty one PhDs and has authored or coauthored

more than one hundred publications in book chapters and scientific journals.



Konstantina (Nantia) S. Nikita (M'96-SM'00) received the diploma in Electrical Engineering and the Ph.D. degree from the National Technical University of Athens (NTUA), as well as the M.D. degree from the Medical School, University of Athens. From 1990 to 1996, she worked as a researcher at the Institute of Communication and Computer

Systems. In 1996, she joined the School of Electrical and Computer Engineering, NTUA, as an assistant professor, and since 2005, she serves as a professor at the same school. Moreover, she is an Adjunct Professor of Biomedical Engineering and Medicine, Keck School of Medicine and Viterbi School of Engineering, University of Southern California. She has authored or co-authored 165 papers in refereed international journals, 41 chapters in books and over 300 papers in international conference proceedings. She is editor of seven books in English and author of two books in Greek. She holds two patents. She has been the technical manager of several European and National R&D projects. She has been honorary chair/chair of the program/organizing committee of several international conferences, and she has served as keynote/invited speaker at international conferences, symposia and workshops organized by NATO, WHO, ICNIRP, IEEE, URSI, etc. She has been the advisor of 27 completed Ph.D. theses, several of which have received various awards. Her current research interests include biomedical telemetry, biological effects and medical applications of radiofrequency electromagnetic fields, biomedical signal and image processing and analysis, simulation of physiological systems, and biomedical informatics. She is Associate Editor of the IEEE Transactions on Biomedical Engineering, the IEEE Journal of Biomedical and Health Informatics, the IEEE Transactions on Antennas and Propagation, the Wiley Bioelectromagnetics and the Journal of Medical and Biological Engineering and Computing. She has received various honors/awards, with the Bodossakis Foundation Academic Prize (2003) for exceptional achievements in "Theory and Applications of Information Technology in Medicine" being one of them.

She has been a member of the Board of Directors of the Atomic Energy Commission and of the Hellenic National Academic Recognition and Information Center, as well as a member of the Hellenic National Council of Research and Technology. She has also served as the Deputy Head of the School of Electrical and Computer Engineering of the NTUA. She is a member of the Hellenic National Ethics Committee, a Founding Fellow of the European Association of Medical and Biological Engineering and Science (EAMBES), a Fellow of the American Institute of Medical and Biological Engineering (AIMBE) and a member of the Technical Chamber of Greece and of the Athens Medical Association. She is also a member of the BHI Technical Committee, the founding chair and ambassador of the IEEE-EMBS, Greece chapter and has served as vice chair of the IEEE Greece Section.